The Journal of Antibiotics (2017), 1–6

www.nature.com/ja

NOTE

Isolation and structure elucidation of lipopeptide antibiotic taromycin B from the activated taromycin biosynthetic gene cluster

Kirk A Reynolds[1,2,5], Hanna Luhavaya[1,5], Jie Li[1], Samira Dahesh[3], Victor Nizet[3,4], Kazuya Yamanaka[1,6] and Bradley S Moore[1,4]

In the ongoing effort to unlock the chemical potential of marine bacteria, genetic engineering of biosynthetic gene clusters (BGCs) is increasingly used to awake or improve expression of biosynthetic genes that may lead to discovery of novel bioactive natural products. Previously, we reported the successful capture, engineering and heterologous expression of an orphan BGC from the marine actinomycete *Saccharomonospora* sp. CNQ-490, which resulted in the isolation of the novel lipopeptide antibiotic taromycin A. Herein we report the isolation and structure elucidation of taromycin B, the second most abundant product of the taromycin biosynthetic series, and show that taromycins A and B exhibit complex chromatographic properties indicative of interconverting conformations. Taromycins A and B display potent activity against methicillin-resistant *Staphylococcus aureus* and vancomycin-resistant *Enterococcus faecium* clinical isolates, suggestive that the taromycin molecular scaffold is a promising starting point for further derivatization to produce compounds with promising antibiotic characteristics.
The Journal of Antibiotics advance online publication, 29 November 2017; doi:10.1038/ja.2017.146

Lipopeptide molecules as a source for novel bioactivity have received consistent interest as a source of antibiotics. The earliest recognition of lipopeptide potential came with the isolation and characterization of amphomycin (**1**) (Figure 1), a potent calcium-dependent antibiotic.[1] First characterized in 1953 from *Streptomyces canus*, **1** was active against Gram-positive bacteria through the disruption of cell wall synthesis.[2] Although the bioactivity of **1** was notable, its tendency to induce hemolysis prevented its clinical use as an antibiotic.[3] Following the discovery of **1**, the lipopeptide class of antibiotics has continued to expand, significantly culminating in the Food and Drug Administration approval and commercial success of daptomycin (**2**) (Figure 1).[4]

Structurally, lipopepide antibiotics are characterized by a central cyclic decapeptide core with additional exocyclic amino acids terminating in a fatty acid side chain. A wide diversity of lipid side chains has been observed, including differences in chain length, degree of unsaturation and configuration.[5] In addition to the lipid side chain, the bioactivity of lipopeptides has been observed to be highly dependent on their ability to bind calcium within cell walls. The nature of this relationship has been demonstrated with the lipopeptide daptomycin.[6] The aspartic acid residue Asp-7 allows for coordination of Ca^{2+} in a 1:1 stoichiometric ratio, resulting in daptomycin aggregation in the cytoplasmic membrane of Gram-positive bacteria.[7]

In the ongoing effort to combat antibiotic resistance, the robust bioactivity and success of daptomycin has renewed interest in the antibiotic potential of lipopeptides. Previously, we reported the discovery of a silent biosynthetic gene cluster (BGC) from the marine bacterium *Saccharomonospora* sp. CNQ-490 with strong homology to the daptomycin BGC.[8] Following capture and heterologous expression of this novel BGC in the *Streptomyces coelicolor* M1146 host, we described the isolation and structure elucidation of the most abundant secondary metabolite in the series, the chlorinated lipopeptide taromycin A (**3**).[8] Following this initial discovery, we began our investigation of other products of the taromycin BGC. Described herein is the isolation and structure elucidation of taromycin B (**4**), a new analog of the taromycin series produced by heterologous expression of the activated taromycin BGC.

LC-MS analysis of ethyl acetate extracts of *S. coelicolor* M1146-M1 cultures showed a complex profile comprised of at least 10 peaks with isotopic distribution consistent with dichlorinated taromycin A analogs (Figure 2a, Supplementary Figure S1).[8] MS and MS/MS analysis of peaks 1 and 3 indicated the addition of oxygen on the central peptide ring. These analogs were not present in initial extracts and grew in abundance over time, thereby indicating peaks 1 and 3 were oxidation artifacts. Peaks 2, 4 and 5 all exhibited identical MS

[1]Scripps Institution of Oceanography, University of California at San Diego, La Jolla, CA, USA; [2]Department of Chemistry and Biochemistry, University of California at San Diego, La Jolla, CA, USA; [3]Department of Pediatrics, University of California at San Diego, La Jolla, CA, USA and [4]Skaggs School of Pharmacy and Pharmaceutical Sciences, University of California at San Diego, La Jolla, CA, USA
[5]KA Reynolds and H Luhavaya contributed equally to this work.
[6]Current address: Department of Life Science and Biotechnology, Kansai University, Suita, Osaka, Japan.
Correspondence: Professor BS Moore, Scripps Institution of Oceanography, University of California at San Diego, 9500 Gilman Drive MC 0204, La Jolla, CA 92093-0204, USA.
E-mail: bsmoore@ucsd.edu
Received 17 May 2017; revised 20 October 2017; accepted 25 October 2017

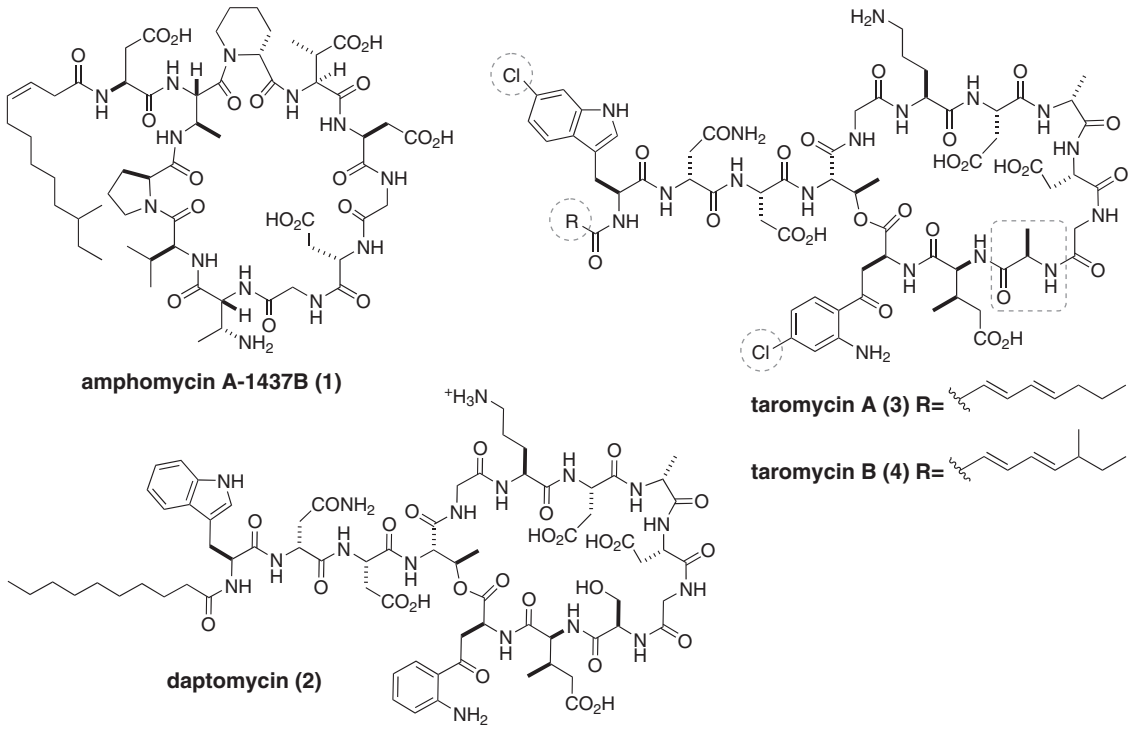

Figure 1 Chemical structures of compounds **1**–**4**. Key structural differences between **3**, **4** and **2** are marked by dashed lines.

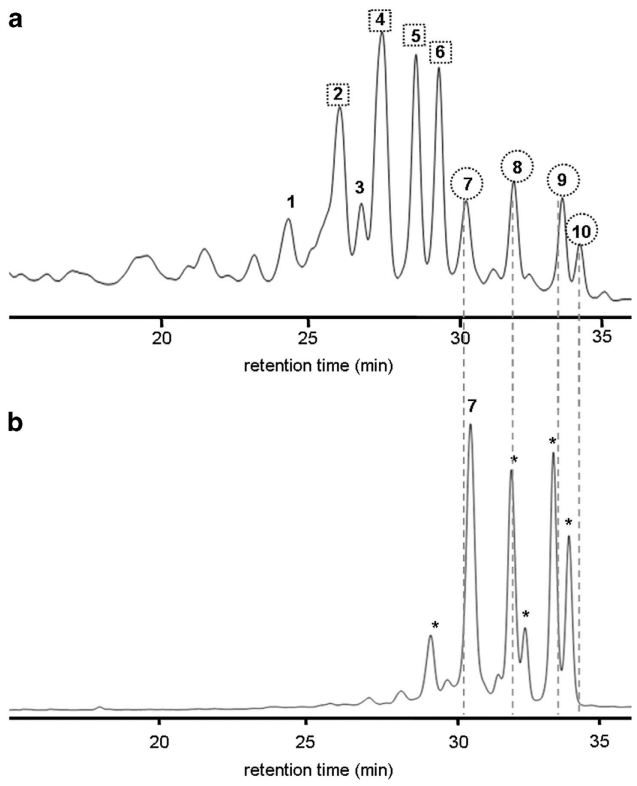

Figure 2 (**a**) HPLC-MS trace of crude extract of taromycin-producing strain. Peaks 2, 4–6: taromycin A, peaks 7–10: taromycin B. (**b**) Isolated peak 7 from the above trace yields peaks 7–10 (**m/z* 1654.55) upon re-injection. A full color version of this figure is available at The Journal of Antibiotics journal online.

and MS/MS fragmentation patterns to compound **3** (originally isolated from peak 6),[8] while peaks 7–10 similarly all showed *m/z* 1654.553 consistent with a methylated analog of **3**. Throughout this article, we refer to series with *m/z* 1640.583 as taromycin A (**3**) and to series with *m/z* 1654.553 as taromycin B (**4**). The location of the methylation on the new taromycin analog was of interest as methylation on the acyl side chain could affect the molecule's ability to congregate in the cell wall. Alternatively, methylation on the core peptide could affect Ca^{2+} binding, which in turn may also affect the molecule's antibiotic properties. As both situations have precedence in other lipopeptide series,[9] we further explored the structure of the methylated taromycin analog.

Following the collection of four chromatographic peaks corresponding to *m/z* 1640.583 and four peaks with *m/z* 1654.553, each of the isolated peaks was re-evaluated by LC-MS and MS/MS analyses. LC-MS data revealed that re-injection of any individual peak with *m/z* 1654.553 resulted in a mixture that reproduced peak distributions 7–10 (Figure 2b, Supplementary Figure S3). We similarly analyzed individually isolated peaks 2, 4, 5 and 6 (*m/z* 1640.583), and once again in each case, we consistently observed the appearance of the same family of four peaks with nearly identical distribution (Supplementary Figure S3). The observed interconversion of peaks suggested the equilibrium of different conformational forms of the two taromycin molecules under experimental conditions.

Compounds **3** (7 mg) and **4** (3 mg) were purified from 2 liter of culture of the *S. coelicolor* M1146-M1 strain (Supplementary Information). Even though the peak splitting was observed for the isolated fractions, only fractions corresponding to peak 6 for taromycin A and peak 7 for taromycin B were used to perform structure elucidation. High-resolution MS^n analysis of **4** by ESI-time of flight and Fourier Transform ion cyclotron resonance MS showed identical peptide core MS fragmentation to that of the compound **3**, indicating

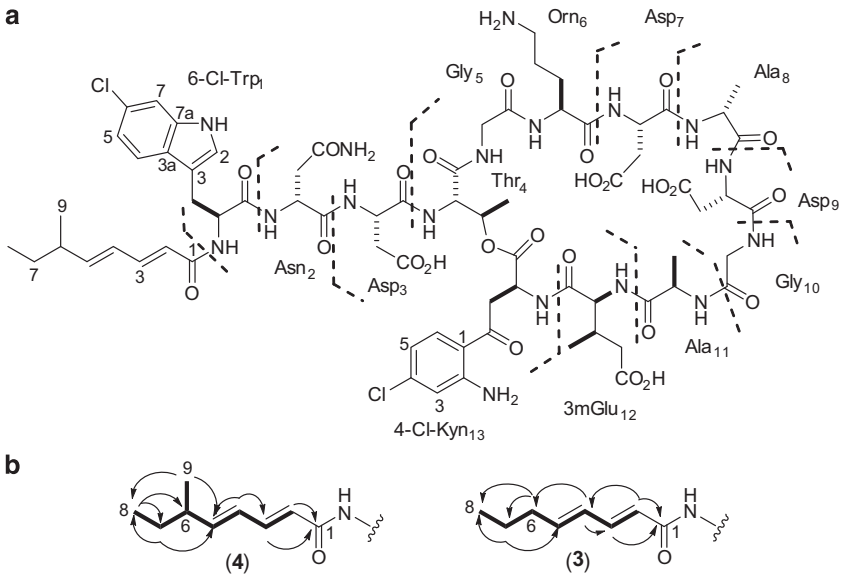

Figure 3 (**a**) High-resolution MS/MS analysis of **4**. (**b**) Key ^{1}H-^{1}H COSY (—) and ^{1}H-^{13}C HMBC (→) correlations in fatty acid moiety of compounds **4** and **3**.

that the two molecules share the same amino-acid sequence (Figure 3, Supplementary Figure S2, Supplementary Table S1). The only observed fragmentation difference was found to be on the exocyclic acyl side chain. A structural difference on the acyl side chain corresponds to what has been observed with the natural lipopeptides from the daptomycin-producer *Streptomyces roseosporus*, where the acyl side chains ranged in chain length, unsaturation and methylation pattern.[10]

The structure **4** was then established by comprehensive analysis of one- and two-dimentional NMR spectroscopic data and comparison to those of taromycin A (**3**) and daptomycin (Table 1, Supplementary Figure S4).[11] The locations of the chlorine atoms on the tryptophan and kynurenine residues in **4** were confirmed by HSQC and COSY correlations. The chlorine atoms were found to be on the C-4 and C-6 positions of the kynurenine and tryptophan residues, respectively, consistent with **3** (Table 1). The structure of the exocyclic lipid chain was determined by COSY, HSQC and HMBC NMR correlations (Figure 3b, Table 1). The lipid side chain is eight carbons in length with a methyl branch at the anteiso position (C-6) and similar to that in **1**. In addition, the lipid side chain of **4** has two unsaturations at C-2 and C-4, as observed for **3**. Although the side chain is branched, the presence of exclusively C_8 chains in the taromycin series may indicate strong selectivity within the taromycin biosynthetic pathway. This would be a departure from the C_{11}, C_{12} and C_{13} chains observed in the natural lipopeptides produced by *S. roseosporus*.[9] Acyl chain selectivity remains challenging to predict from comparative genomic sequencing due to the high degree of freedom associated with long carbon chains. To date, the challenge of acyl chain selectivity has only been successfully investigated through co-crystallization of substrate alkyl chains with their respective enzyme partners.[12,13]

The stereochemistry of taromycin A (**3**) was previously determined by Marfey analysis, and the constituent amino acids were found to be of identical stereochemistry to that of daptomycin.[8] Owing to the biosynthetic and structural relatedness of **3** and the methylated analog **4**, we anticipated that they would share similar optical properties. We measured the optical rotation of **4** ($[\alpha]_D^{20} = +4.53^{o}$) and compared that against those of **3** ($[\alpha]_D^{20} = +4.52^{o}$) and **2** ($[\alpha]_D^{20} = +4.78^{o}$), thereby confirming that all the molecules share the same configurations. The stereochemistry of the C-9 methyl group, however, was not determined, though biosynthetically the acyl side chain likely begins with a stereoisomer of isoleucine.[14]

During early bioactivity optimization studies, it was found that the C_{10} carbon side chain of daptomycin greatly contributes to its potent antibiotic activity.[10] With **3** showing modest bioactivity[8] (Table 2), the structural differences in **4** offer another opportunity to study the structure–activity relationship in this structural series. Among the antibiotic-resistant pathogens of interest to our study is the highly clinically relevant methicillin-resistant *Staphylococcus aureus* (MRSA). Taromycin B was found to have minimum inhibitory concentration values identical to taromycin A against three different MRSA strains tested in this study (Table 2). Daptomycin continues to have the most potent bioactivity of the three molecules, further emphasizing the importance of the C_{10} side chain.

In addition to MRSA, we also tested compound **4** against clinically relevant strains of vancomycin-resistant *Enterococcus faecium* (VRE), a major opportunistic pathogen that is known to cause infections in hospitalized patients. Taromycin B was also determined to have identical minimum inhibitory concentration values to taromycin A against three VRE clinical isolates (Table 2). It was again the case that daptomycin was found to have the most potent activity against VRE strains.

Although the bioactivity of taromycin B does not match that of daptomycin, literature precedence indicates that taromycin B may show significant bioactivity potential. As described earlier, the length and saturation of the acyl side chain has a critical role in the bioactivity of daptomycin. During the development of daptomycin, numerous side chains were added to the core daptomycin peptide to optimize bioactivity.[9] During those early studies, it was found that C_8 daptomycin had an minimum inhibitory concentration of 8 μg ml^{-1} against *S. aureus*.[9] Taromycin B showed activities of 3.1 and 12.5 μg ml^{-1} against the daptomycin-sensitive MRSA strains tested, which is comparable to C_8 daptomycin and indicative of the potential for structure-based optimization of antibiotic activity using this scaffold.

In summary, the heterologous expression of the activated taromycin BGC has yielded a second molecule in the lipopeptide series,

Table 1 NMR spectroscopic data for compounds 3 and 4 in DMSO-*d6*, 600 MHz

		*Taromycin A (**3**)*		*Taromycin B (**4**)*	
Residue	*Position*	*δH mult. (J)*	*δC*	*δH mult. (J)*	*δC*
6-Cl-Trp_1	NH	8.14[a]	—	8.24[a]	—
	α-CH	4.46 br d	54.6	4.46 br d	54.8
	β-CH_2	2.95 d (9.4) 3.05 d (12.7)	27.3	2.95 d (10.5) 3.05 d (11.2)	27.2
	1 (NH)	10.34 br s	—	10.35 br s	—
	2	7.21 s	125.5	7.21 br s	125.4
	3	—	110.5	—	110.7
	3a	—	126.6	—	126.7
	4	7.6 d (8.2)	120.4	7.60 d (8.3)	120.3
	5	6.97 br d	119.1	6.97 d (8.3)	119.0
	6	—	—[b]	—	—[b]
	7	7.37[a]	111.5	7.37[a]	111.4
	7a	—	136.9	—	136.6
	C=O	—	172.0	—	171.8
Asn_2	NH	7.96[a]	—	7.94[a]	—
	α-CH	4.52[a]	50.3	4.52[a]	50.5
	β-CH_2	2.52 m	36.4	2.57 m	36.3
	C=O	—	170.4	—	172.2
	$CONH_2$	—[b]	173.7	—[b]	176.8
Asp_3[c]	NH	8.29[a]	—	8.14[a]	—
	α-CH	4.64 m	49.7	4.64 m	49.8
	β-CH_2	2.49[a]	36.8	2.41[a]	37.5
	C=O	—	171.1	—	170.8
	COOH	—	172.7	—	173.5
Thr_4	NH	7.97[a]	—	7.97[a]	—
	α-CH	4.54 br d	55.4	4.53 br d	55.0
	β-CH	5.14 m	70.8	5.14 m	70.9
	y-CH_3	1.05[a]	16.1	1.05[a]	16.1
	C=O	—	171.9	—	171.4
Gly_5[c]	NH	8.09[a]	—	8.12[a]	—
	α-CH_2	3.83 br s	42.5	3.83 br s	42.4
	C=O	—	—[b]	—	—[b]
Orn_6	NH	8.14[a]	—	8.18[a]	—
	α-CH	4.19 m	53.0	4.18 m	53.1
	β-CH_2	1.76 m	28.5	1.75[a]	28.6
	γ-CH_2	1.63 m	23.6	1.61 m	23.9
	δ-CH_2	2.85[a]	38.9	2.82[a]	38.9
	NH_2	7.81[a]	—	7.79[a]	—
	C=O	—	172.0	—	172.3
Asp_7[c]	NH	8.51[a]	—	8.17[a]	—
	α-CH	4.62 m	50.2	4.61 m	49.8
	β-CH_2	2.41[a]	37.2	2.37[a]	37.4
	C=O	—	171.4	—	172.1
	COOH	—	174.3	—	174.3
Ala_8[c]	NH	7.99[a]	—	7.96[a]	—
	α-CH	4.23 m	49.1	4.23 m	49.0
	β-CH_3	1.23[a]	18.3	1.22[a]	18.2
	C=O	—	172.1	—	172.7
Asp_9[c]	NH	8.29[a]	—	8.29[a]	—
	α-CH	4.66 m	49.8	4.60 m	49.8
	β-CH_2	2.51[a]	35.6	2.55[a]	36.6
	C=O	—	170.8	—	171.6
	COOH	—	173.1	—	173.8
Gly_{10}[c]	NH	8.29[a]	—	8.05[a]	—
	α-CH_2	3.64 m, 3.68 m	42.2	3.72 m, 3.76 m	42.3
	C=O	—	171.7	—	171.5
Ala_{11}[c]	NH	8.02[a]	—	8.06[a]	—
	α-CH	4.40[a]	48.9b	4.40[a]	48.9
	β-CH_3	1.24 d (5.6)	18.2	1.20[a]	18.2

Table 1 (Continued)

		*Taromycin A (**3**)*		*Taromycin B (**4**)*	
Residue	*Position*	*δH mult. (J)*	*δC*	*δH mult. (J)*	*δC*
	C=O	—	172.4	—	172.6
$3mGlu_{12}$	NH	7.98[a]	—	7.93[a]	—
	α-CH	4.53[a]	55.4	4.52[a]	55.6
	β-CH	2.36 m	33.4	2.35 m	33.6
	$γ-CH_2$	1.89[a]	38.7	1.89[a]	38.9
	$γ-CH_3$	0.84[a]	14.4	0.83 br d	14.5
	C=O	—	171.1	—	—[b]
	COOH	—	173.9	—	173.7
4-Cl-Kyn_{13}	NH	8.35[a]	—	8.40[a]	—
	α-CH	4.78 m	48.7	4.78 m	48.6
	$β-CH_2$	3.49[a], 3.56[a]	40.1	3.48[a], 3.56[a]	40.1
	γ(C=O)	—	197.7	—	197.4
	1	—	115.9	—	115.7
	2	—	152.4	—	152.3
	3	6.85 br d	116.1	6.85 br d	116.0
	4	—	139.1	—	138.9
	5	6.56 d (7.9)	115.0	6.55 d (8.2)	114.9
	6	7.82[a]	134.1	7.81[a]	134.1
	C=O	—	171.4	—	171.0
	NH_2	—[b]	—	—[b]	—
C_8	1 (C=O)	—	166.5	—	166.3
	2	5.66 br d	119.5	5.64 br d	119.5
	3	6.30 br d	127.9	6.32 br d	141.3
	4	7.35[a]	141.3	7.33[a]	128.8
	5	5.86 m	142.9	5.76 m	138.7
	6	2.06 (CH_2) m	34.6	2.07 (CH) m	38.4
	7	1.35 m	21.9	1.30 m	29.4
	8 (CH_3)	0.84[a]	14.2	0.80[a]	14.7
	9 (CH_3)	NA	NA	0.93 d (7.2)	19.8

Abbreviations: br, broad, NA, not applicable.
All assignments were made on the basis of ^1H, COSY, HSQC and HMBC data (δ in p.p.m., *J* in Hz).
[a]Overlapped signals.
[b]Not observed.
[c]Interchangeable assignment between the same amino-acid residue types.

Table 2 Taromycin A (3), taromycin B (4) and daptomycin (2) minimum inhibitory concentrations (MIC) (50 μg ml^{-1} $CaCl_2$)

	MIC, μg ml^{-1}		
Strain	*2*	*3*	*4*
MRSA A8819-DapS	2.5	3.1	3.1
MRSA A8817-DapR	>10	50	50
MRSA0325	>10	12.5	12.5
VRE5938	>10	50	50
VRE 447-DapS	5	12.5	12.5
VRE 447-DapR	>10	50	>100

Abbreviations: DapR, daptomycin resistant; DapS, daptomycin susceptible; MRSA, methicillin-resistant *Staphylococcus aureus*; VRE, vancomycin-resistant *Enterococcus faecium*.
OD600<0.04 is considered minimum inhibitory concentration.

taromycin B. This new taromycin analog contains the hallmark 6-chloro-trypophan and 4-chloro-kynurenine residues and is structurally differentiated by methyl branching found on the acyl side chain. Upon chromatographic analyses of isolated taromycin A and B molecules, the appearance of multiple peaks with identical masses was observed. Based on analysis presented here, we propose that these numerous analogs are primarily comprised of two taromycin derivatives; however, additional experiments are required to clarify the structural features that give rise to their suspected conformational differences. Both derivatives, however, have C_8 chains, indicating that the lack of diversity in chain length found within the taromycin series is unique when compared with the variety of chain lengths found within the natural daptomycin producer *S. roseosporus*, implying greater specificity in taromycin biosynthesis. Taromycin B was found to have antibiotic activity against both *S. aureus* and *E. faecium*, though the bioactivity did not match or surpass that of daptomycin. Finally, the taromycin series expands upon our understanding of the chemical potential found in microbial silent gene clusters.

CONFLICT OF INTEREST

The authors declare no conflict of interest.

ACKNOWLEDGEMENTS

We are grateful to PR Jensen and W Fenical for providing *Saccharomonospora* sp. CNQ-490, M Bibb for *S. coelicolor* M1146, RD Kersten for assistance with MS analysis, BM Dungan for assistance with NMR, X Tang and PA Jordan for helpful discussions. This work was supported by grants from the National Institutes of Health (R01-GM085770 to BSM, U01-AI124316 to VN and Instrument Grant S10-OD010640).

DEDICATION

Dedicated to the special issue celebrating Professor KC Nicolaou for his great scientific contribution to total synthesis of highly complex and biologically important natural products.

1 Heinemann, B., Kaplan, M. A., Muir, R. D. & Hooper, I. R. Amphomycin, a new antibiotic. *Antibiot. Chemother.* **3**, 1239–1242 (1953).
2 Tanaka, H., Oiwa, R., Matsukura, S., Inokoshi, J. & Omura, S. Studies on bacterial cell wall inhibitors. X. Properties of phospho-N-acetylmuramoyl-pentapeptide-transferase in peptidoglycan synthesis of *Bacillus megaterium* and its inhibition by amphomycin. *J. Antibiot.* **35**, 1216–1221 (1982).
3 Yang, H.-J. *et al.* Two novel amphomycin analogues from *Streptomyces canus* strain FIM-0916. *Nat. Prod. Res.* **28**, 861–867 (2014).
4 Eisenstein, B. I., Oleson, F. B. Jr. & Baltz, R. H. Daptomycin: from the mountain to the clinic, with essential help from Francis Tally, MD. *Clin. Infect. Dis.* **50**, S10–S15 (2010).
5 Mnif, I. & Ghribi, D. Review lipopeptides biosurfactants: mean classes and new insights for industrial, biomedical, and environmental applications. *Biopolymers* **104**, 129–147 (2015).
6 Ball, L.-J. *et al.* NMR structure determination and calcium binding effects of lipopeptide antibiotic daptomycin. *Org. Biomol. Chem.* **2**, 1872–1878 (2004).
7 Micklefield, J. Biosynthesis and biosynthetic engineering of calcium-dependent lipopeptide antibiotics. *Pure Appl. Chem.* **81**, 1065–1074 (2009).
8 Yamanaka, K. *et al.* Direct cloning and refactoring of a silent lipopeptide biosynthetic gene cluster yields the antibiotic taromycin A. *Proc. Natl Acad. Sci.* **111**, 1957–1962 (2014).
9 Debono, M. *et al.* Enzymatic and chemical modifications of lipopeptide antibiotic A21978C: the synthesis and evaluation of daptomycin (LY146032). *J. Antibiot.* **41**, 1093–1105 (1988).
10 Huber, F. M., Pieper, R. L. & Tietz, A. J. The formation of daptomycin by supplying decanoic acid to *Streptomyces roseosporus* cultures producing the antibiotic complex A21978C. *J. Biotechnol.* **7**, 283–292 (1988).
11 Gu, J. Q. *et al.* Structural characterization of a lipopeptide antibiotic A54145E (Asn3Asp9) produced by a genetically engineered strain of *Streptomyces fradiae*. *J. Antibiot.* **64**, 111–116 (2011).
12 Agarwal, V., Lin, S., Lukk, T., Nair, S. K. & Cronan, J. E. Structure of the enzyme-acyl carrier protein (ACP) substrate gatekeeper complex required for biotin synthesis. *Proc. Natl Acad. Sci.* **109**, 17406–17411 (2012).
13 Cryle, M. J. & Schlichting, I. Structural insights from a P450 Carrier Protein complex reveal how specificity is achieved in the P450BioI ACP complex. *Proc. Natl Acad. Sci.* **105**, 15696–15701 (2008).
14 Li, Q. *et al.* Deciphering the biosynthetic origin of L-allo-isoleucine. *J. Am. Chem. Soc.* **138**, 408–415 (2016).

Supplementary Information accompanies the paper on The Journal of Antibiotics website (http://www.nature.com/ja)